SEMI-ACTIVE VIBRATION CONTROL BASED ON SHAPE MEMORY ALLOY ACTUATORS – ANALYSIS AND EXPERIMENTAL TESTING

Jaakko Heinonen, Ismo Vessonen
Paul Klinge, Tomi Lindroos

Journal of Structural Mechanics,
Vol. 40, No. 1, 2007, pp. 23-38

SUMMARY

Vibration control of civil structures, machines or generators for instance, is a challenging task when the structure undergoes various loading conditions from normal operation to extreme loadings like earthquake. Adaptive vibration control for changes in environmental and operational conditions is capable of achieving optimum performance in all circumstances. In this study, new numerical methods and novel applications for semi-active vibration isolators were developed. The basic idea was to control the stiffness by changing the kinematic boundary condition of the device. After numerical studies, two different concepts were developed: a circular frame spring and a cylindrical elastomer spring. The stiffness control was actuated by shape memory alloy (SMA) material embedded into the device. Both concepts were verified experimentally.

INTRODUCTION

This work was carried out in VTT´s technology theme: Intelligent Products and Systems under the topic Embedded Structural Intelligence. The objective in this topic is to cost-efficiently embed intelligence into structures, which can enable utilization of entirely new types of product concepts with high performance and reliable operation. The key focus area is to develop functional materials, and affordable wireless measurement technology and control, which are adaptable to operating conditions, and to apply these in vibration, durability and shape control.

A semi-active device supporting a structure or machine at its base or a part of a structural joint can be utilized to isolate vibrations. In a semi-active isolator, the stiffness and/or damping can be controlled during operation. Changing the stiffness of the support device can be exploited by moving the eigenfrequency of the system to bypass the resonance. Reliable control of the support device requires monitoring a critical point of the structure and knowledge about the frequency response of the system. This kind of adaptive isolator can change operation conditions according to the dominant loading, resulting in improved vibration isolation capability compared to passive systems. Undesired vibrations can be reduced in different loading conditions, i.e. a large frequency range is covered.

The paper firstly introduces the principles of semi-active vibration control demonstrated by a single degree of freedom system (mass-spring-dashpot). Secondly, a "smart element" is presented, which was developed to describe the semi-active characteristics of vibration isolators for finite element simulation purposes. Thirdly, some practical solutions for semi-active vibrations isolators based on the shape memory alloy (SMA) material are introduced. The basic idea was to control the stiffness by changing the kinematic boundary condition of the device. Various innovations were simulated and some of them tested experimentally.

PRINCIPLES OF SEMI-ACTIVE VIBRATION CONTROL

A semi-active system is one whose dynamic properties can be adjusted in response to a command signal, which offers the possibility to exert a large control effort with little energy input. This is useful in many applications compared to *a passive system* in which the characteristics are fixed and to *an active system*, which acts on its environment using energy from another source. The semi-active control can be utilized for real-time tuning of the stiffness or damping during continuous action (Srinisavan and McFarland, 2001).

Semi-active vibration control is demonstrated by the single degree of freedom (sdof) system shown in Fig. 1. A rigid mass supported by a translational stiffness and dashpot was loaded by a harmonic force. An analytical solution for a response in forced harmonic loading was introduced, for instance, by Tedesco et al. (1999).

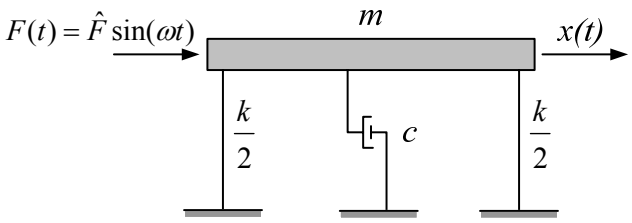

Figure 1. Vibrating single degree of freedom system. Only the horizontal degree of freedom is considered. The mass m = 100 kg, viscous damping coefficient c = 400 Ns/m, force amplitude $\hat{F} = 500\,\mathrm{N}$

Utilizing the semi-active vibration isolator for translational stiffness in Fig. 1, one can characterize the maximum controllable stiffness region by defining a stiffness ratio κ as

$$\kappa = \frac{k^{(2)}}{k^{(1)}} \tag{1}$$

in which k is the stiffness and the superscript in parenthesis describes the mode, while the vibration isolation device is acting in soft (1) and stiff (2) operation modes.

A displacement amplitude for the sdof system as a function of the loading frequency in steady-state vibration is defined as (Tedesco et al., 1999)

$$\hat{x} = \frac{\hat{F}/k}{\sqrt{\left(1-r^2\right)^2 + \left(2\zeta r\right)^2}} \tag{2}$$

in which ζ is a damping factor (the fraction of the critical damping) and r is a frequency ratio. They are defined as

$$\zeta = \frac{c}{2m\omega_n}\ , \qquad r = \frac{\omega}{\omega_n}\ , \qquad \omega_n = \sqrt{\frac{k}{m}} \tag{3}$$

where c is the viscous damping coefficient, ω is the circular loading frequency and ω_n is the circular eigenfrequency of the corresponding undamped system.

In semi-active stiffness control, the stiffness of the system is changed. The basic idea is to measure and analyze the structure response continuously. When the structure undergoes an excitation close to the eigenfrequency, the resonance vibration can be avoided by changing the stiffness to move the eigenfrequency of the system. The response spectrum must be known beforehand to make a decision on whether the stiffness needs to be increased or decreased.

Two different cases are considered in which the stiffness can be controlled between 40 and 200 kN/m, i.e. the stiffness ratio of the vibration isolator is 5. In the first case, the vibration isolator operates initially in the soft mode and the structure is loaded by harmonic force at a frequency of 2.4Hz. The stiffness was controlled from soft to stiff mode. In the second case, the vibration isolator operates initially in the stiff mode and the structure is loaded by harmonic force at a frequency of 7.5Hz. The stiffness was controlled from stiff to soft mode. The corresponding eigenfrequencies in the soft and stiff modes are 3.2Hz and 7.1Hz. The displacement responses in steady-state vibration for the sdof system are shown in Fig. 2 for both cases. The damping was considered constant.

In both loading conditions, 2.4 Hz and 7.5 Hz loading frequency, the displacement response decreased significantly owing to the stiffness control, as shown in Fig. 2. This is a useful concept in this idealized sdof example when the loading frequency varies in different loading conditions. In practical applications, the system usually consists of a large number of dofs, and the system has several eigenfrequencies which requires a more advanced control algorithm to achieve the desired vibration mitigation. Also, in the case of wide-band excitation, the influence of semi-active control is not obvious. In this case, one promising control strategy is to continuously change the stiffness to bypass the steady-state resonance vibration.

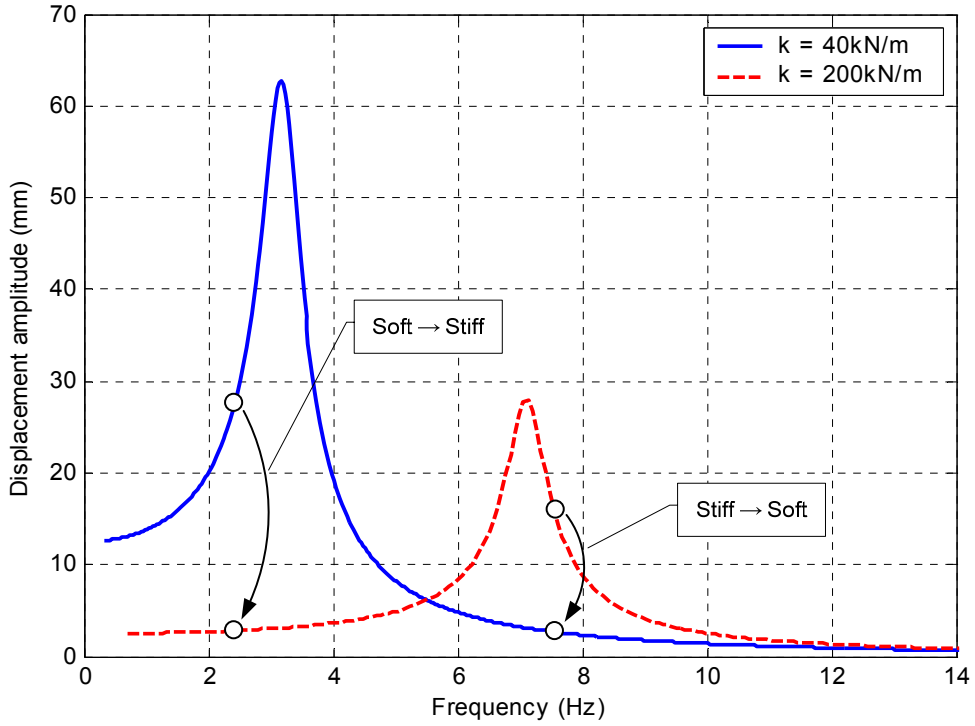

Figure 2. Displacement amplitude in the sdof system as a function of the loading frequency with different stiffness.

SEMI-ACTIVE ISOLATOR ELEMENT IN FINITE ELEMENT METHOD

General

A "smart element" was developed to describe the semi-active characteristics of vibration isolators for structural analysis purposes. The numerical analyses were conducted using the commercial finite element method (FEM) software ABAQUS/Standard. A semi-active vibration isolator can be applied in ABAQUS/Standard either by utilizing connector elements existing in the code or by developing a user element subroutine to define the desired properties for an isolator element.

The connector element is used to define a connection between two nodes (or between one node and the ground) and it can be used to incorporate simple spring, dashpot and friction elements into one single element. The connector behaviour can be linear or non-linear. In the semi-active control, the connector properties are adjusted during the simulation. For instance, the deformation, acceleration or stress in the selected point of structure can be used as variables for the feedback algorithm. In ABAQUS, the user can create a user subroutine (UFIELD) to evaluate solution-dependent field variables to be used for the control. Updating connector element behaviour for every time increment in dynamic analysis results in an explicit method, because element behaviour is constant

during the time increment. Therefore, a short time increment is needed to avoid cumulative error during the direct time integration procedure.

Another way to model a semi-active isolator in ABAQUS is to create a user element subroutine (UEL), which is useful in modelling active control mechanisms (ABAQUS, 2001a). UEL can be connected with other elements in the structural model and the results are easily read during the post processing. The benefit of using the user element subroutine becomes obvious when a complicated feedback algorithm needs to be modelled.

Principles for programming

The main issues in programming a UEL subroutine in the case of static or dynamic analysis are defining the nodal forces and stiffness matrix based on the displacement degrees of freedom. The nodal forces and stiffness matrix are computed at the element level in every time increment and iteration. In addition, any solution-dependent state variables associated with the user element need to be updated. The principles for developing and programming the UEL subroutine for different analysis procedures in ABAQUS/Standard are introduced next (ABAQUS, 1997, 2001a, 2001b, Belytschko et al., 2000).

Generally, in static analysis the user needs to define the nodal forces and the element stiffness matrix for each user element in every time increment and iteration. One can apply a virtual work principle and finite element discretization to obtain the nodal forces F^N in the element, symbolically defined as

$$F^N = F^N_{ext} - F^N_{int} \tag{4}$$

in which F^N_{ext} is the external equivalent nodal force (traction and volume forces) and F^N_{int} is the internal nodal force due to stresses. All forces might be solution-dependent. External solution-independent nodal forces are not described in the UEL subroutine because they do not contribute to the element stiffness. The nodal force F^N is called the "nodal residual force" by ABAQUS to describe that the solution for the global equilibrium equations in the numerical procedure is found by setting the residual force at each dof equal to zero.

The solution of the nonlinear system of equations in ABAQUS requires that the element stiffness matrix K^{MN} (Jacobian) is defined as

$$K^{NM} = -\frac{\mathrm{d}F^N}{\mathrm{d}u^M} = -\frac{\partial F^N}{\partial H^\alpha}\frac{\partial H^\alpha}{\partial u^M} \tag{5}$$

in which the stiffness matrix depends on the displacement u^M and internal state variables H^α. The Jacobian should contain all dependencies between F^N and u^M to improve

convergence in the nonlinear analysis. With regard to the eigenfrequency analysis, the Jacobian must be correct.

In direct-integration dynamic analysis, ABAQUS uses the Hughes-Hilber-Taylor time integration scheme completed by Newmark formulae for displacements and velocity integration. In this case, the nodal residual forces have the form

$$F^N = -M^{NM}\ddot{u}_{t+\Delta t} - (1+\alpha)\left(F^N_{ext} - F^N_{int}\right)_{t+\Delta t} + \alpha\left(F^N_{ext} - F^N_{int}\right)_t \tag{6}$$

where $t+\Delta t$ is time at the end of the increment. Respectively, t is the time at the beginning of the increment. The Jacobian J^{NM} (tangential stiffness matrix in the dynamic nonlinear analysis) has the form

$$J^{NM} = M^{NM}\left(\frac{\mathrm{d}\,\ddot{u}}{\mathrm{d}\,u}\right) + (1+\alpha)C^{NM}\left(\frac{\mathrm{d}\,\dot{u}}{\mathrm{d}\,u}\right) + (1+\alpha)K^{NM} \tag{7}$$

where M^{NM} is the mass matrix, C^{NM} is the damping matrix and K^{NM} is the element stiffness matrix defined in Eq. (5). One should observe that the mass matrix is defined to include all derivatives of $\ddot{u}$ and the damping matrix all derivatives of $\dot{u}$.

$$M^{NM} = -\frac{\mathrm{d}\,F^N}{\mathrm{d}\,\ddot{u}^M} \qquad \text{and} \qquad C^{NM} = -\frac{\mathrm{d}\,F^N}{\mathrm{d}\,\dot{u}^M} \tag{8}$$

Parameters $\mathrm{d}\ddot{u}/\mathrm{d}u$, $\mathrm{d}\dot{u}/\mathrm{d}u$ and α follow from the Hughes-Hilbert-Taylor integrator operator and they are passed into the user element subroutine as:

$$\frac{\mathrm{d}\,\ddot{u}}{\mathrm{d}\,u} = \frac{1}{\beta\Delta t^2}, \quad \frac{\mathrm{d}\,\dot{u}}{\mathrm{d}\,u} = \frac{\gamma}{\beta\Delta t}, \quad \beta = \frac{1}{4}(1\text{-}\alpha)^2, \quad \gamma = \frac{1}{2} - \alpha, \quad \frac{1}{3} \le \alpha \le 0 \tag{9}$$

where the parameter α describes the amount of numerical damping. If automatic time incrementation is used, the user needs to define also the half-step residual force in the subroutine (ABAQUS, 2001b).

Element implementation

A general spring-dashpot user element with two nodes was created, as shown in Fig. 3. The mass of the smart isolator element can be modelled by the overlaying mass element.
The degrees of freedom are the nodal displacements in the global coordinate system. In addition, the first and second time derivative of dof at the end of the time increment is passed into UEL.

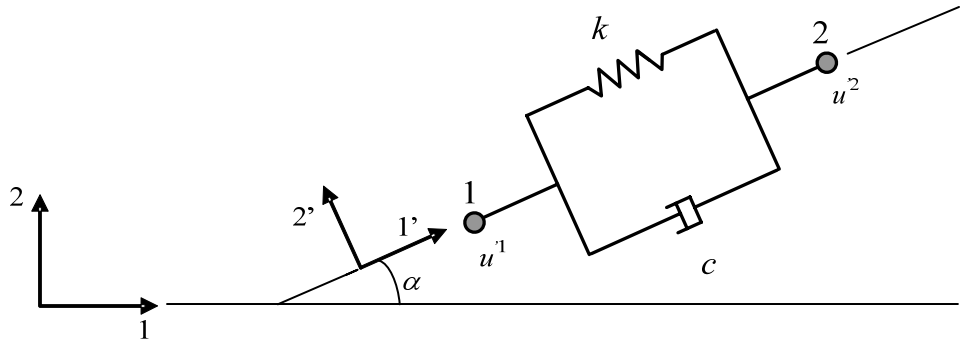

Figure 3. A connector element containing a spring and dashpot.

The internal connector force F_{int} has the following simple form

$$F_{int} = ku + cv \tag{10}$$

where the stiffness k and damping coefficient c can be solution-dependent. u and v are the relative displacement and velocity along the line between nodes 1 and 2 ($u = u'^2 - u'^1$, $v = \dot{u}'^2 - \dot{u}'^1$). Equation (10) can be modified to take into account the frictional force to model dissipation and hysteresis in loading loops (Heinonen, 2006b).

The formulation with nodal variables in the global coordinate system needs coordinate transformation. The nodal displacement vector in the global coordinate system **u** is transformed into the local system **u'** by using a transformation matrix **T** (Cook et al., 1989)

$$\mathbf{u}' = \mathbf{T}\mathbf{u} \tag{11}$$

in which the transformation matrix contains direction cosines. The same transformation is written in the component form as

$$\begin{Bmatrix} u'^1 \\ u'^2 \end{Bmatrix} = \begin{bmatrix} \cos\alpha & \cos\beta & \cos\gamma & 0 & 0 & 0 \\ 0 & 0 & 0 & \cos\alpha & \cos\beta & \cos\gamma \end{bmatrix} \begin{Bmatrix} u_x^1 \\ u_y^1 \\ u_z^1 \\ u_x^2 \\ u_y^2 \\ u_z^2 \end{Bmatrix} \tag{12}$$

where α, β and γ are the angles between the connector line and the global coordinate axis (x, y and z).

The local stiffness matrix **K`** is written as

$$\mathbf{K}' = k' \begin{bmatrix} 1 & -1 \\ -1 & 1 \end{bmatrix} \tag{13}$$

where k' is the axial stiffness according to Eq. (7). The stiffness matrix in the global coordinate system is

$$\mathbf{K} = \mathbf{T}^T \mathbf{K}' \mathbf{T} \tag{14}$$

Example

The applicability of the smart element in semi-active vibration control is demonstrated in a time domain by the same sdof system shown previously with the same loading cases (a harmonic load with 2.4 and 7.5 Hz frequencies). The stiffness control from soft to stiff or vice versa, was conducted after a given number of oscillations, as shown in Fig. 4. By comparing the amplitudes in the time domain to those analyzed in the frequency domain (Fig. 2) one observes equal results. Some variation in the time domain occurs owing to the beating phenomenon.

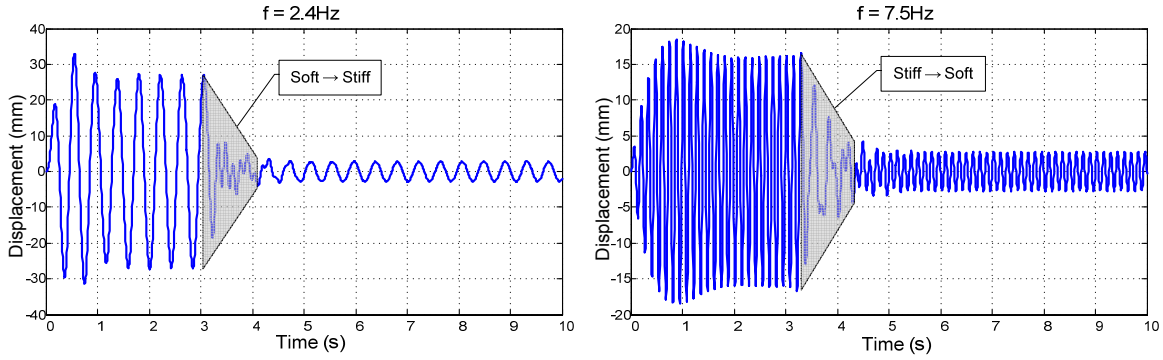

Figure 4. Displacement response of a harmonically loaded sdof system in the time domain during semi-active stiffness control. The shaded area indicates the period for the stiffness control in the simulation.

CONCEPTS FOR SEMI-ACTIVE VIBRATION ISOLATOR

Several different concepts were studied to develop new types of vibration isolators including development of numerical models for semi-active control (Heinonen et al., 2006a and 2006c). The basic idea of semi-active control was to change the kinematic boundary condition in the horizontal direction of the device to adjust its vertical stiffness. Two new concepts were selected for further analysis and experimental demonstrations:

1. A circular metal frame (ring) with a horizontal SMA string
2. An axial elastomer spring attached with a circular SMA support ring

Behaviour of shape memory alloy

The change of boundary condition can be implemented in different ways. As the actuator was made of SMA, it was necessary to study some of the features of SMA material behaviour to develop a semi-active isolator. Shape memory alloys are metals that "remember" their original shapes. The most common types of SMA are nickel-titanium alloys (NiTiX) where X denotes ternary element such as copper (Cu). Binary nickel-titanium alloy M is employed in this study. Shape memory alloys may have different kinds of shape memory effects: one-way shape memory and two-way shape memory. After a sample of one-way SMA has been deformed permanently from its original configuration, its original geometry is restored by itself during heating. The two-way SMA remembers two different shapes: one at low temperature, and one at high temperature. This study is limited to the one-way shape memory alloys.

The mechanical behaviour of SMA material is complicated. Coupling of the stress, strain and temperature depends on the phase transformation between the martensitic and austenitic phase. The phase transformation mainly depends on the temperature but also on the stress, and the transformation is hysteretic (Srinisavan and McFarland, 2001,). At room temperature, the SMA is in martensitic form (low-temperature phase). During heating, the SMA transforms to the austenitic phase (high-temperature phase), as shown in Fig. 5. The temperatures at which the phase transformations take place are identified as M_s, M_f, A_s and A_f. M_s is the temperature at which the martensite phase starts to form and at M_f the phase transformation is over. A_s and A_f are the corresponding temperatures for austenitic transformation. A fraction of martensite ξ is used to measure the phase composition; ξ=1 denotes a fully martensitic phase and ξ = 0 a fully austenitic phase (Srinisavan and McFarland, 2001).

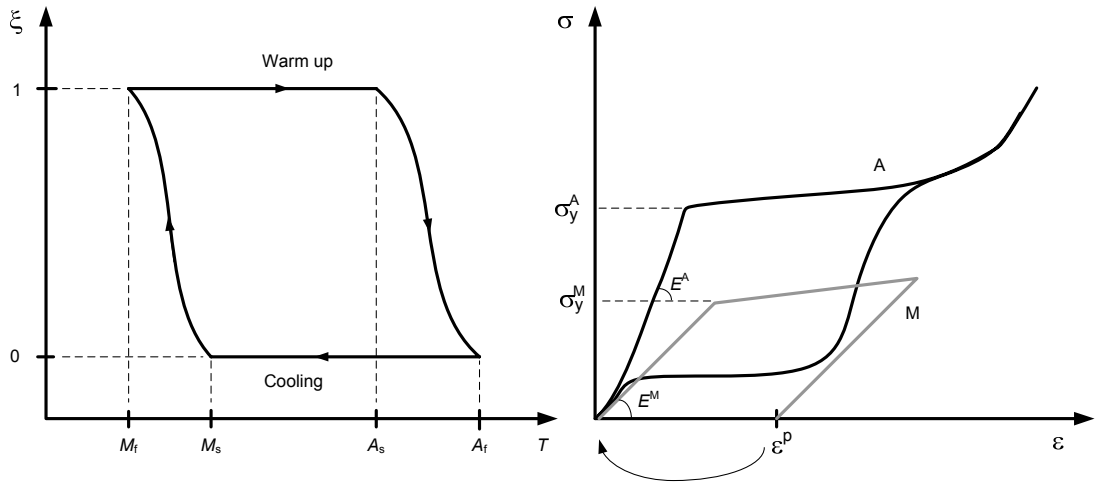

Figure 5. On the left: fraction of martensite ξ as a function of temperature. On the right: schematic presentation of typical stress-strain behaviour of SMA in the austenitic phase (A) and martensitic phase (M). E is the elastic modulus and σ_y is the yield stress (plateau stress) with superscripts indicating the phase. ε^p is the permanent strain that can be recovered during transformation M $\rightarrow$ A.

Figure 5 shows the stress-strain relation of the SMA string in uniaxial loading and unloading. The curves are based on the tensile tests at constant temperature for both phases (Auricchio, 1995). In the austenitic phase (temperature region $A_f - A_f$ +30K), the

SMA is able to recover large strains (up to 8 - 15% depending on the composition of the SMA) and can be characterized as superelastic. In the martensitic phase, the SMA material can be deformed permanently by applying stress that exceeds the yield stress (plateau stress). As a result of the shape memory effect, this deformation can be recovered by heating the SMA owing to transformation from the martensite to austenitic phase. Typical behaviour of NiTi-based SMA is that both the elastic modulus and yield stress are significantly higher in the austenitic phase than in the martensitic phase.

Despite the complicated material behaviour of SMA, several constitutive models have been published, for instance, by Auricchio (1995), Sittner et al. (2000) and Kosel and Videnic (2005). An implementation of constitutive models for a structural analysis purpose has been published by Sippola and Heinonen (2006).

Circular frame spring

The main idea of the controllable device was to change its boundary condition to adjust the stiffness. The selected construction for the device was a circular frame (a ring). While the ring is loaded vertically it behaves as a spring. During the compression the ring expands horizontally, as shown in Fig. 6. Restricting the deformation in the horizontal direction, the stiffness of the frame in the vertical direction becomes higher due to confinement. The change of boundary condition was applied by an SMA string to adjust the gap between the frame and confinement, as shown in Fig. 6. The gap is closed by warming up the SMA. In this case, the frame acts in stiff mode. To activate the operation in the soft mode again, the SMA needs to be loaded enough to exceed the yield stress, which results in permanent deformation to create the gap.

The controllable stiffness ratio of the device from soft to stiff mode was determined to go up to 6.4 (Heinonen et al., 2006a). The influence is caused purely by changing the boundary condition. It does not depend on dimensions or material parameters as long linear elastic material behaviour is valid. By taking into account the compliance of the SMA string, the stiffness ratio is 6.0.

Experimental verification of circular frame spring

After numerical feasibility studies by FEM, two different frame rings were studied experimentally by applying static and dynamic loading tests. The first frame was made of aluminium, and the second one of steel. The diameter for the steel frame was 80mm, the width 10.0 mm and the thickness 0.78mm. Corresponding values for the aluminium frame were 60mm, 10.9mm and 0.84mm.

A dynamic test controlled by constant displacement amplitude was started when the SMA string was at room temperature (22 ºC). The frame was first preloaded sufficiently to ensure that the frame acted in compression only. The SMA was heated resistively by applying a power supply and the temperature of the SMA was measured by a T-type thermocouple and controlled by an analogue PID-regulator (Heinonen et al., 2006a).

The dynamic properties were characterized by varying the temperature, preload and displacement amplitude.

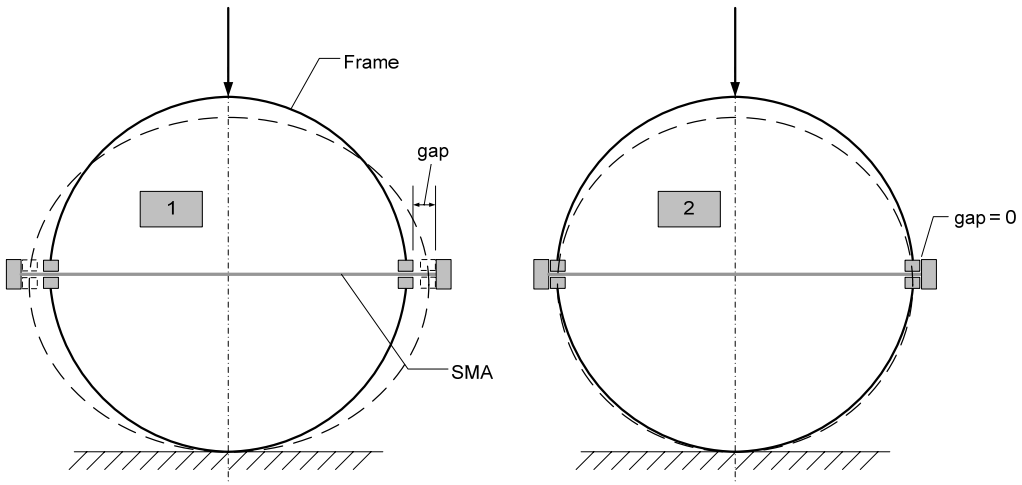

Figure 6. Boundary condition of the frame adjusted by an SMA string controlling the gap. The frame is acting in soft mode on the left (mode 1) and in stiff mode on the right (mode 2). The original state is shown by solid lines, and the deformed state by dashed lines.

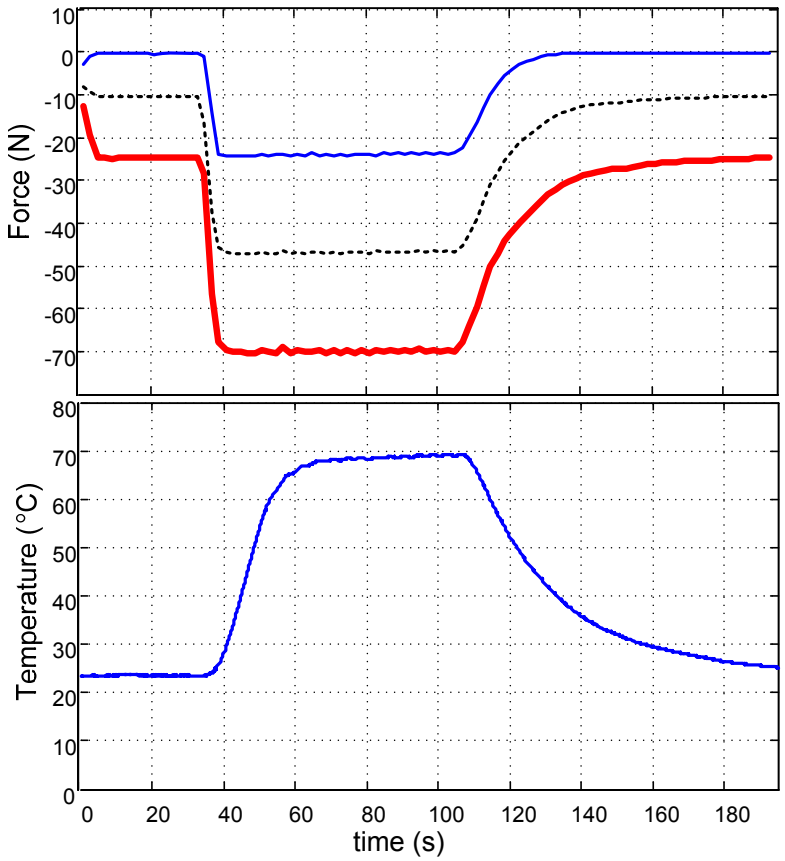

Figure 7. Envelope curves for force in the time domain during the temperature control of the SMA string. The thick red line indicates compression and the thin blue line tension. The average force is shown by the dashed line. A harmonic excitation with constant displacement amplitude 1.0 mm at 0.5 Hz was applied for a steel frame preloaded by 1.0 mm.

The increase of SMA string temperature activated stiff mode and subsequent cooling activated soft mode again, as shown in Fig. 7. Increasing the current passing through the SMA changes the stiffness rapidly, indicating a quick response of the shape memory effect. The stiffness ratio between the stiff and soft mode can be characterized from Fig. 7 by determining the dynamic stiffness from a certain number of loading cycles. The average stiffness ratio was typically from 3.4 to 4.1 but some individual tests showed values of up to 5.0. Although the theoretical value that takes into account the compliance of the SMA string is 6.0, the achieved controllable stiffness range is large enough for many applications.

Elastomer spring

The idea was the same as in the frame spring: to change its boundary condition to adjust the stiffness. The selected construction for the semi-active isolator consisted of two parts, a cylindrical elastomer and SMA actuator. A circular support ring made of SMA was used as an actuator, which was attached to the outside of a cylindrical elastomer spring. The change of boundary condition was controlled by the gap between the elastomer spring and constraint, as shown in Fig. 8. While a cylindrical block of the elastomer is compressed in the vertical direction, it expands in the horizontal direction (perpendicular to the load). Restricting the expansion, the axial stiffness in the loading direction becomes higher. The operation mode, stiff or soft, was selected by controlling the temperature of the SMA actuator which controls the phase composition of SMA.

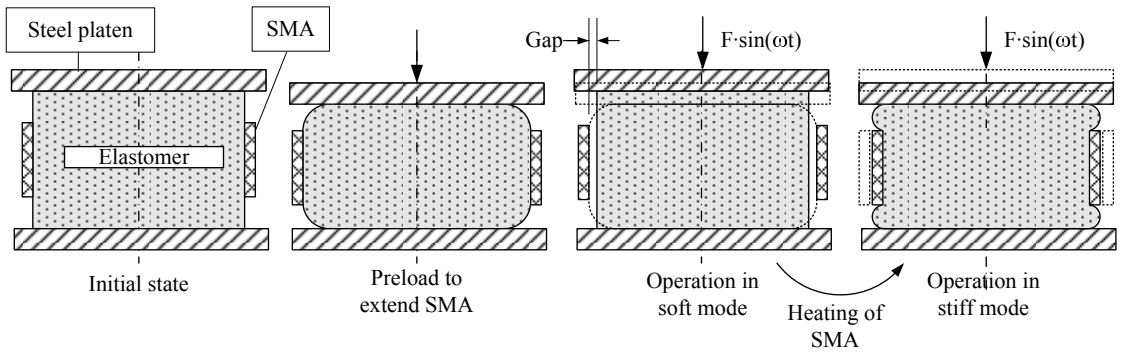

Figure 8. Principal sketch of operation modes of the semi-active device. After preliminary adjustments by preloading, the device acts in two operation modes: soft and stiff.

Numerical studies were made with the FEM (ABAQUS/Standard) to verify the functionality of the device, to design the dimensions and to select appropriate materials to achieve a sufficient stiffness ratio (Heinonen et al., 2006c). The stiffness ratio depends on the geometric shape of the spring and the ratio between the confined area in the stiff mode and the area where the material can expand freely in the soft mode. With suitable design of the spring, the stiffness ratio can be over 10. The influence is purely caused by changing the boundary condition.

Initially, the gap was adjusted equal to zero at room temperature for the SMA ring (constraint) in the martensitic phase. Permanent deformations of the SMA were released by annealing beforehand. Thereafter, the spring was sufficiently loaded vertically to

create permanent deformation to the SMA constraint (ε^p in Fig. 5). The elongation of the SMA constraint created the gap to enable operation in a soft mode. The gap needs to be large enough to prevent closing owing to deformations while the spring is acting in the soft mode.

To change the boundary condition, the gap is closed by warming up the SMA. During transformation M $\rightarrow$ A, the permanent deformation is recovered due to the shape memory effect. In vertical loading, the horizontal deformation is restricted due to confinement applied by the SMA ring. In this case, the spring acts in stiff mode.
Transformation A $\rightarrow$ M is activated by cooling the SMA below M_f temperature. To activate the operation in the soft mode again, external work is needed to load the SMA enough to exceed the yield stress, which results in permanent deformation to create the gap.

Experimental verification of elastomer spring

Polyurethane elastomer (PUR Shore 90) was chosen as a base material. The PUR grade was chosen such that the stiffness did not change significantly in the temperature control region (20–70°C). The elastic modulus was approximately 23 MPa. Nickel-titanium alloy was selected for the SMA in the circular support ring material.

Dynamic loading tests were carried out to verify the feasibility of the semi-active device (Fig. 9). The temperature control of the SMA constraint was applied by an external air blow system in which the air temperature and flow were controlled. The isolator was covered by a stiff plastic cylinder which was slightly larger than the elastomer part to allow the elastomer and SMA constraint deformations. The air was blown into the cylinder through a pipe. The air came out from the gap between the bottom steel platen and the plastic cylinder. The air temperature control was based on three thermal elements located between the SMA constraint and elastomer.

A sinusoidal displacement controlled loading with a constant amplitude and frequency was applied. The amplitude was 0.25 mm and the frequency was 0.5 or 5 Hz in each test. At first, the gap was created by a preload with large amplitude (2 mm) to activate the soft mode. Then in every test, a preload corresponding to 1 mm displacement was applied to ensure that the isolator was under compressive loading in each loading cycle. The temperature of the SMA constraint was controlled to activate first the soft mode and then the stiff mode.

Experimental tests indicated promising results, although the controllable stiffness region was not as high as expected according to the analysis. Figure 9 presents the stiffness during the control of SMA temperature in the low-frequency test (0.5 Hz). Starting from the soft mode, the stiffness was 2.2 kN/mm. Increasing the SMA temperature activated the stiff mode smoothly. The uneven jump at 45ºC was due to the break in tests. A further increase of the temperature made the isolator stiffer. The maximum recorded stiffness was 9.8 kN/mm at 70ºC. The stiffness still showed a slight trend to increase;

however, further values were not recorded. In this example, the maximum stiffness ratio was 4.5.

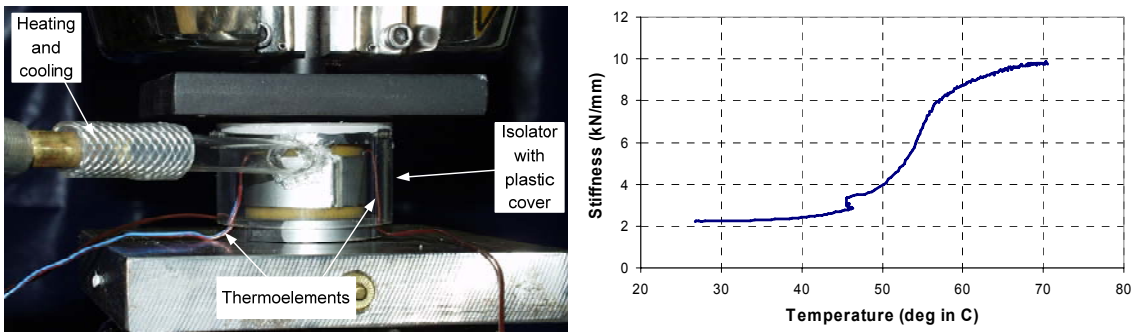

Figure 9. On the left: test set-up for loading tests. On the right: stiffness control from soft to stiff mode during low frequency (0.5 Hz) tests.

FUTURE APPLICATIONS

Vibrations of slender offshore structures that are subjected to the dynamic actions of drifting sea ice are good examples where adaptive vibration can be utilized. As a basic solution, these structures will have a conical waterline geometry that prevents the most severe problem known as self-induced vibration due to level ice. It is proposed that the remaining vibrations can be solved by additional control devices. The prospects of using a semi-active tuned mass damper or semi-active smart cone to mitigate vibrations in offshore wind turbines has been studied numerically by Kärnä et al. (2004) and by Mroz and Kärnä (2005).

CONCLUSIONS

In this study, principles for semi-active vibration control were demonstrated by a single degree of freedom system. A new numerical subroutine was developed to describe a semi-active isolator element for finite element simulation purposes. The model can be utilized in structural analysis to study influences of semi-active control in the time domain.

Novel applications for semi-active vibration isolators were developed. The basic idea was to change the kinematic boundary condition by embedding a shape memory alloy actuator into the device. After studying a considerable number of innovations, two different concepts were developed further: a circular frame spring and a cylindrical elastomer spring. Experimental tests for both concepts indicated promising results. Although the controllable stiffness region was not as high as expected, the current solutions create a good foundation for future developments.

ACKNOWLEDGMENT

Dr. Tuomo Kärnä is acknowledged for all his support and comments. Mr. Erkki Järvinen, Mr. Juha Juntunen and Mr. Mats Rundt are acknowledged for all their help in the tests and data analysis. Mr. Kari Kolari is acknowledged for the review and comments.

REFERENCES

ABAQUS (1997), Theory Manual Version 5.7, Hibbitt, Karlsson, Sorensen, Inc.

ABAQUS (2001a), Writing User Subroutines with ABAQUS, Course material, Hibbitt, Karlsson, Sorensen, Inc., Lectures held in Espoo Finland 10.9-11.9.2002

ABAQUS (2001b) User's Manual Vol. 1, 2 and 3, Version 6.2, , Hibbitt, Karlsson, Sorensen, Inc.

Auricchio F., Shape Memory Alloys: Applications, Micromechanics, Macromodelling and Numerical Simulations, Doctoral thesis, 1995, University of California at Berkeley, 163 p.

Belytschko T., Liu W.K. and Moran B. Nonlinear Finite Elements for Continua and Structures, Chichester: Wiley, 650 p., ISBN: 0-471-98774-3, 2000

Cook, R.D., Malkus, D.S, Plesha M.E., Concepts and Applications of Finite Element Analysis, 3rd edition, John Wileys & Sons, Singapore, 1989, 630 p., ISBN 0-471-50319-3

Heinonen J., Kärnä T., Vessonen I., Klinge P. and Järvinen E., Controlling Stiffness of a Frame Spring by Changing the Boundary Condition with an SMA Actuator, Submitted to Computers & Structures (accepted), 2006 (a)

Heinonen J., Preliminary Study of Modelling Dynamic Properties of Magnetorheological Fluid Damper, VTT Working Papers : 45, VTT, Espoo 2006 (b). 36 p., ISBN 951-38-6597-5

Heinonen J., Kärnä T., Vessonen I., Klinge P. and Lindroos T., Semi-active Vibration Isolator Based on Elastomer Material Controlled by an SMA actuator, Proceedings of the Fifth International Conference on Engineering Computational Technology, Edited by: B.H.V. Topping, G. Montero and R. Montenegro (CST 2006), Civil-Comp Press, Stirlingshire, Scotland, paper 98, 2006 (c)

Kosel, F. and Videnic, T., Generalized Plasticity and Uniaxial Constrained Recovery in Shape Meory Alloys, II Eccomas Thematic Conference on Smart Structures and Materials, C.A. Mota Soares et al. (Eds.), Lisbon, Portugal, July 18-21, 2005

Kärnä, T.; Kolari, K.; Heinonen, J., Mitigation of Dynamic Ice Actions on Offshore Wind Turbines, Proceedings of the Third European Conference on Structural Control, 3ECSC, Vienna, Austria, 12-15 July 2004. Vienna University of Technology. Vienna (2004)

Mroz, A.; Kärnä, T., Mitigation of ice loading. Feasibility study of semi-active solution. http://www.vtt.fi/inf/pdf/workingpapers/2005/W39.pdf, 2005. VTT, Espoo. 34 p. VTT Working Papers: 39

Sippola, M., Heinonen, J.: Muistimetallimateriaalimallien implementointi Matlab- ja ABAQUS-ohjelmiin (in Finnish). Research report VTT-R-07220-06, Espoo, 2006, 30 p.

Sittner P., Stalmans R. and Tokuda M., An algorithm for prediction of the hysteretic responses of shape memory alloys, Smart Materials and Structures, 9 (2000) 452-465

Srinisavan A.V. and McFarland D.M., Smart Structures, Analysis and Design, 2001, Cambridge University Press, ISBN 0-521-65026-7, 228 p.

Tedesco, J.W., McDougal, W.G., Ross. C.A., Structural dynamics : theory and applications, Addison-Wesley, Menlo Park, CA. 1999, 816 p. ISBN: 0-673-98052-9

Jaakko Heinonen, senior research scientist
VTT Technical Research Centre of Finland
P.O. Box 1000, FIN-02044 VTT, Finland
Email: jaakko.heinonen@vtt.fi

Ismo Vessonen, senior research scientist
VTT Technical Research Centre of Finland
P.O. Box 1000, FIN-02044 VTT, Finland
Email: ismo.vessonen@vtt.fi

Paul Klinge, senior research scientist
VTT Technical Research Centre of Finland
P.O. Box 1000, FIN-02044 VTT, Finland
Email: paul.klinge@vtt.fi

Tomi Lindroos, research scientist
VTT Technical Research Centre of Finland
Box 1000, FIN-02044 VTT, Finland
Email: tomi.lindroos@vtt.fi